Rocznik Ochrona Środowiska

Volume 25 Year 2023 ISSN 2720-7501 pp. 16-24

https://doi.org/10.54740/ros.2023.003 open access

Received: March 2023 Accepted: March 2023 Published: April 2023

Determination of the Specific Heat Flux During Boiling of the Dispersed Phase of the Emulsion

Anatoliy Pavlenko[1], Hanna Koshlak[2], Borys Basok[3], Tatiana Hrabova[4]*

[1]Kielce University of Technology, Poland

https://orcid.org/0000-0002-8103-2578

[2]Kielce University of Technology, Poland

https://orcid.org/0000-0001-8940-5925

[3]Institute of Engineering Thermophysics of the National Academy of Sciences of Ukraine, Ukraine

https://orcid.org/0000-0002-8935-4248

[4]Institute of Engineering Thermophysics of the National Academy of Sciences of Ukraine, Ukraine

https://orcid.org/0000-0002-5194-2474

[*]corresponding author's e-mail:apavlenko@tu.kielce.pl

Abstract: The intensity of heat exchange between the boiling emulsion and the enclosing surfaces is associated with the physical phenomena of the formation, growth, and destruction of vapour bubbles of the low-boiling component in the liquid phase. This article presents a methodology to assess the intensity of heat exchange processes. Using this technique, it is possible to predict the energy parameters of heat exchange equipment and the degree of intensification of heat transfer processes.

Keywords: steam explosion, homogenisation, boiling, intensification of heat, and mass transfer

1. Effects of Intense Heat Transfer in Liquid Mixtures

The intensity of heat exchange processes during contact of the emulsions with a low-boiling dispersed phase with the surfaces of the heat exchangers depends on the characteristics of the emulsions and heat transfer processes in the flow structure and at the contact boundary with the surface. An important factor is the formation of vapour bubbles in superheated drops to estimate the specific heat flux value. The degree of incompleteness of the transition of a boiling drop from a homogeneous liquid to a homogeneous vapour state greatly determines heat transfer efficiency.

When the temperature of the heating wall is higher than that of saturated vapours of the dispersed low-boiling phase, the droplets are overheated near the pipeline wall, which contributes to the appearance of steam nuclei in their volume.

It is known that when heating emulsions with a continuous medium, in contrast to homogeneous liquids, it is associated with the so-called delayed boiling of the dispersed phase, which expands the range of the bubble boiling regime (Albanese et al. 2019, Adhikari et al. 2016, Dietzel et al. 2017, Gasanov & Bulanov 2015, Dąbek et al. 2018, Dąbek et al. 2019). In this case, the temperature of the heating surface Tn can be much higher than that of saturated vapours Tsat of the dispersed phase, reaching a difference of one hundred or more degrees and preventing the transition to the film boiling mode. In (Chandrapala et al. 2012, Badve et al. 2012, Ganesan et al. 2015, Feng et al. 2015, Pavlenko 2018), the boiling of emulsions is presented based on the classical mechanisms of boiling in an unlimited volume of homogeneous liquids, focussing on the study of the effect of solid microscopic particles in a superheated liquid on the activation of boiling centres. In real heat and mass transfer (HMT) processes, a dispersed low-boiling phase should be considered as a means of initiating centres of vaporisation during the explosive destruction of drops and the formation of vapour-phase bubbles of critical size. Obviously, this effect must be associated with a developed interfacial interface with a high-boiling continuous medium, which mediates heat transfer from the heating surface. The boiling process cannot be limited to heat transfer only, without explicitly considering momentum transfer, particularly viscous shear stresses at high emulsion flow velocity gradients in the near-wall zone near a solid surface.

The study of even only one of the boiling modes, a steam explosion, i.e. a very rapid increase in pressure in a closed volume, and fine fragmentation (crushing) of large fractions of a hot liquid, which ensures this vapourisation, has not yet led to unambiguous ideas about the mechanisms of these physical phenomena (Chernin & Val 2017, Sun et al. 2021, Koshlak & Pavlenko 2019). Each of these processes, which has arisen, stimulates the development of another process. This interconnectedness of the processes of triggering and fine fragmentation – their "conjugation" – significantly complicates the identification of individual, specific fea-

tures of each of them and introduces uncertainty into their description even within the framework of phenomenological approaches. These subprocesses are microseconds, or at best, tens of microseconds. Therefore, to determine the specific heat flux in emulsions, systematic analytical studies of physical phenomena that intensify the HMT processes during emulsions' boiling are necessary.

2. Increasing the Vapour Volume of a Boiling Drop of Emulsion

During the evaporation process, energy is expended both from the side of the low-boiling dispersed phase and from the side of the base liquid, for example, water and oil in an oil-in-water emulsion. Therefore, the temperatures of water and oil will decrease if no heat is supplied to the volume of the emulsion.

The change in the temperature of the oil volume Tm can be determined by the emulsion's total volume, the content of water and oil in it, the size of the droplets of the dispersed phase, and their number. If a certain volume V is given, which contains 30% dispersed water ($V_w = 0.3 \cdot V$) and 70% oil, then to determine the number of particles of the dispersed phase, you can use the particle size distribution histograms. If we assume that the entire dispersed phase will be uniformly distributed in a volume with particles of the same size, then the number of particles in the dispersed phase is equal to

$$N = \frac{3V_w}{4\pi R^3}, \tag{1}$$

where R is the average dispersion of the emulsion, and V – is the volume of the emulsion.

Then the change in oil temperature over time

$$\frac{dT_o}{d\tau} = 4\pi R_4^2 N \frac{q_o}{c_{oil} m_{oil}}, \tag{2}$$

where m_{oil} is the mass, c_{oil} – heat capacity of the carrier phase (oil).

For example, for an emulsion volume $V = 0.5 \cdot 10^{-3}$ m^3 30% water (together with steam), the number of particles with a size $R = 100$ μm is $N = 3.58 \cdot 10^7$ pcs. The results of evaluating the boiling dynamics of such a drop of water located in an infinite volume of oil were performed using the technique presented in the works (Pavlenko 2019, Pavlenko & Koshlak 2021) and in Fig. 1-3.

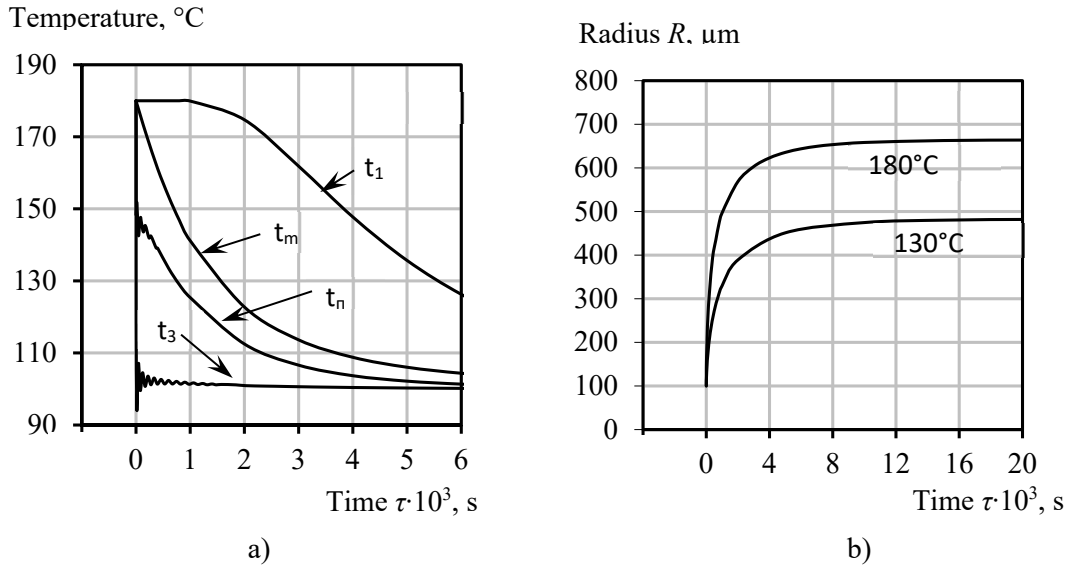

Fig. 1. Changes in temperatures of interfaces t_3, the centre of the water droplet t_1, steam t_n and oil t_m over time at an initial temperature of 180°C (a), as well as changes in the radius of the oil-steam interface at different initial temperatures (b) over time

As seen in Fig. 1a, the oil temperature decrease is more intense than the in the temperature of the centre of the water drop decrease t_1, which is a consequence of the more intense heat transfer from the oil to the steam than from the centre of the water drop to the water-steam interface. This is how heat and mass transfer processes proceed far from the heat exchanger's heating surface. The heat flow from oil to steam and the mass flow are shown in Fig. 2, 3.

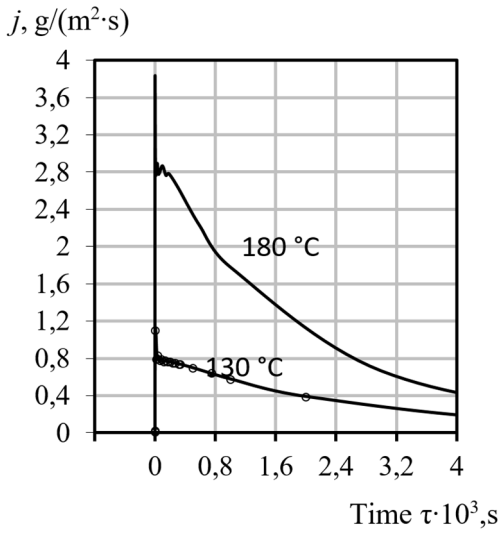

Fig. 2. Change in the specific mass flow over time

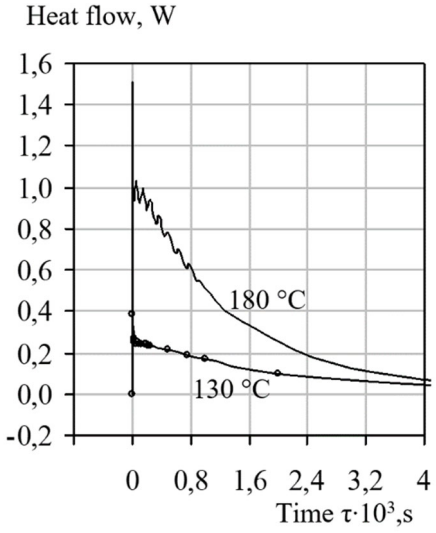

Fig. 3. Change in heat flow from oil to steam over time

As t_m decreases, all the parameters shown in the figures decrease, asymptotically approaching zero, indicating the dominant role of the heat flux Qoil in the heat transfer process. The maximum calculated value of Q_{oil} reaches ≈ 1.5 W per particle. Considering that the number of particles is $N = 3.58 \cdot 10^7$, we can conclude that the heat transfer process is very intense. In this case, fragmentation of the dispersed phase and merging neighbouring emulsion drops are possible. In any case, this will lead to the intensification of heat and mass transfer processes.

Otherwise, heat and mass transfer processes are realised near the heat exchanger's heating surface, where the base fluid's temperature is the same. Figures 4 and 5 show graphs of the specific mass flow and the heat flow versus time. The same conditions were adopted for the calculation, but it was assumed that the temperature of the contact surface (oil) is constant and equal to 180°C. The steam is even more superheated than during the growth of the steam volume away from the heating surface. Its temperature will constantly increase, starting from the moment of practically balanced steam pressure. This fact can be explained by the fact that the heat flow from oil to steam will exceed the effect of the expansion of the steam volume throughout time, as well as the heat flow from steam to water and the heat of the mass flow.

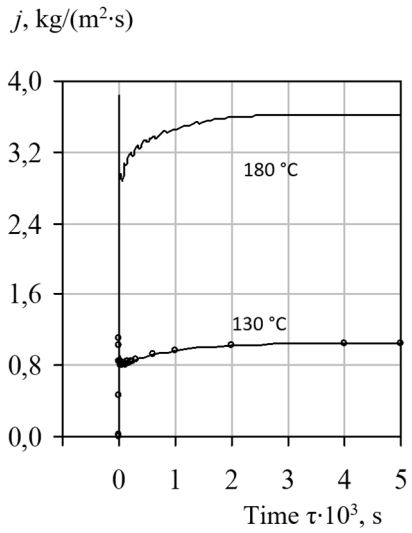

Fig. 4. Change in the specific mass flow over time

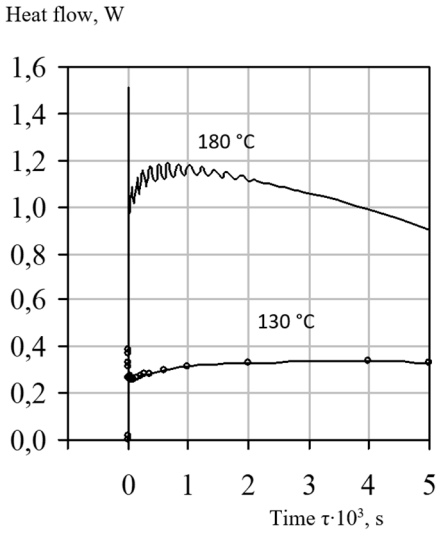

Fig. 5. Change in the heat flow from oil to steam

The difference between heat and mass transfer processes near the heating surface and heat and mass transfer in the emulsion volume is that the volume of steam increases until all of the water has evaporated. The phase transition can be explosive and is accompanied by significant flow turbulence in the near-wall region. This, of course, increases the intensity of heat transfer. The same processes in the emulsion volume can also contribute to an increase in the intensity of HMT. However, the issue of the influence of neighbouring vapour formations

on the dynamics of vapour phase growth, which together create a complex hydrodynamic situation in the oil volume, remains unclear. If the volume of the emulsion moves in the flow, then deformations of the vapour volume occur, which can lead to its separation from the water surface and crushing of the water drop itself. The dynamic parameters of the oil-steam interface in the presence of, for example, three particles, one of which is located between the other two, under conditions of their uneven boiling, can lead to Rayleigh-Taylor or Kelvin-Helmholtz instabilities (Pavlenko et al. 2014a, Pavlenko et al. 2014b). As a result, probably, there will be a breakdown of the steam volume and the destruction of a drop of water. The conditions under which these phenomena are realised are presented in the works (Xun et al. 2020, Bao et al. 2020).

3. Heat and Mass Transfer in the Volume of a Boiling Emulsion.

The complex physicochemical phenomena that determine the stability of thin separating liquid films and the structure of two-phase flows are currently not fully understood. In the volume of a boiling emulsion, the grinding and coalescence of drops are possible. When the drops merge into a conglomerate, the parameters are averaged. The consequence is the appearance of a larger droplet with its own growth rates and accelerations, as well as the determining parameters. Consider two particles of different sizes that merge and determine the parameters of the resulting particle.

The volume of water contained in each particle

$$V_{w_i} = \frac{4}{3}\pi R_i^3, i = 1,2. \tag{3}$$

Mass of water

$$m_{w_i} = V_{w_i}\rho, \tag{4}$$

were:
ρ – the density of water.

Total volume and mass of water

$$V_{w_\Sigma} = \sum_{i=1}^{2}\frac{4}{3}\pi R_i^3, m_w = V_{w_\Sigma}\rho. \tag{5}$$

To determine the temperature of the water formed by the particles, we determined the average temperatures over the cross-section of the water droplets of the initial particles. With a known number of calculated divisions of the cross-section of a water drop and known temperatures in each layer from these divisions, the average temperature of the water volume of each initial particle is determined by the expression

$$t_{m_i} = \frac{\sum_{n=1}^{N_i} t_{n_i}}{N_i}, \tag{6}$$

where N_i is the number of divisions of a given cross-section of the volume of water particles.

The total volume of water determines the radius of the resulting water drop.

$$R_s = \left(\frac{3}{4\pi}V_{w_\Sigma}\right)^{\frac{1}{3}}. \tag{7}$$

The volume of steam in each particle

$$V_{steam_i} = \frac{4}{3}\pi\left(R_{steam_i}^3 - R_i^3\right), i = 1,2. \tag{8}$$

The total radius of the resulting emulsion drop

$$R_\Sigma = \left(\frac{3}{4\pi}V_{n_\Sigma} + R^3\right)^{\frac{1}{3}}. \tag{9}$$

The amount of heat transferred from oil to steam can be determined from the heat balance.

To determine the speed of movement of the oil-vapour interface w_Σ, we add the kinetic energies of the movement of these boundaries of each initial particle. The kinetic energy of each particle is given by

$$E_{k_i} = \frac{1}{2}\rho_{м}\int_{R_\Sigma}^{\infty} 4\pi w^2 r^2 dr = 2\pi\rho_{oil} w_\Sigma^2 R_\Sigma^3, \tag{10}$$

Then the speed w_Σ is

$$w_\Sigma = h\sqrt{\frac{\left|\sum_{i=1}^{2} E_{k_i}\right|}{R_\Sigma^3}}, \tag{11}$$

where:
h – coefficient equal to

$$h = \begin{cases} 1, \sum E_{k_i} \geq 0; \\ -1, \sum E_{k_i} < 0. \end{cases} \tag{12}$$

Coordinates of the centre of the new drop

$$d\left(x_{1,2}, y_{1,2}\right)' = \frac{m_{в_2} + m_{n_2}}{\left(m_{в_1} + m_{n_1}\right) + \left(m_{в_2} + m_{n_2}\right)} d\left(x_{1,2}, y_{1,2}\right), \tag{13}$$

where:
$d\left(x_{1,2}, y_{1,2}\right)'$ – distance from the centre of drop 1 to the centre of a new drop;
$d\left(x_{1,2}, y_{1,2}\right)$ – distance from the centre of drop 1 to the centre of drop 2.

We introduce the notation

$$M = \frac{m_{в_2} + m_{n_2}}{\left(m_{в_1} + m_{n_1}\right) + \left(m_{в_2} + m_{n_2}\right)} = \frac{m_{вn_2}}{\sum_{i=1}^{2} m_{вn_i}}. \tag{14}$$

Then, taking into account the consideration of the geometric theory of the similarity of triangles, we obtain the coordinates of the centre of the new drop

$$x = \left(x_2 - x_1\right)M + x_1, \; y = \left(y_2 - y_1\right)M + y_1. \tag{15}$$

The projections of the velocity vector of the formed drop on the axes are determined using the momentum theorem:

$$w_{kx} = \frac{\left(m_{вn_1} w_{k_1} \sin\gamma_1 + m_{вn_2} w_{k_2} \sin\gamma_2\right)}{m_{вn_1} + m_{вn_2}} = \frac{\sum_{i=1}^{2} m_{вn_i} w_{k_i} \sin\gamma_i}{\sum_{i=1}^{2} m_{вn_i}};$$

$$w_{ky} = \frac{\sum_{i=1}^{2} m_{вn_i} w_{k_i} \cos\gamma_i}{\sum_{i=1}^{2} m_{вn_i}}. \tag{16}$$

Then the velocity of the formed droplet is equal to

$$w_k = \sqrt{w_{kx}^2 + w_{ky}^2}. \tag{17}$$

The new angle will determine the direction of the drop γ

$$\gamma = \begin{cases} arctg\left|\frac{w_{kx}}{w_{ky}}\right|, \frac{w_{kx}}{w_{ky}} \geq 0; \\ 180 - arctg\left|\frac{w_{kx}}{w_{ky}}\right|, \frac{w_{kx}}{w_{ky}} < 0; \\ 90, w_{ky} = 0. \end{cases} \quad (18)$$

Thus, equations (3-18) make it possible to determine the parameters of a newly formed drop.

As an example, let us perform the calculation for the emulsion fragment shown in Fig. 6 at t = 105°C, taking into account the forces that can cause instability, the forces that cause movement, i.e. taking into account the displacement along the axes, as well as taking into account the merging of drops.

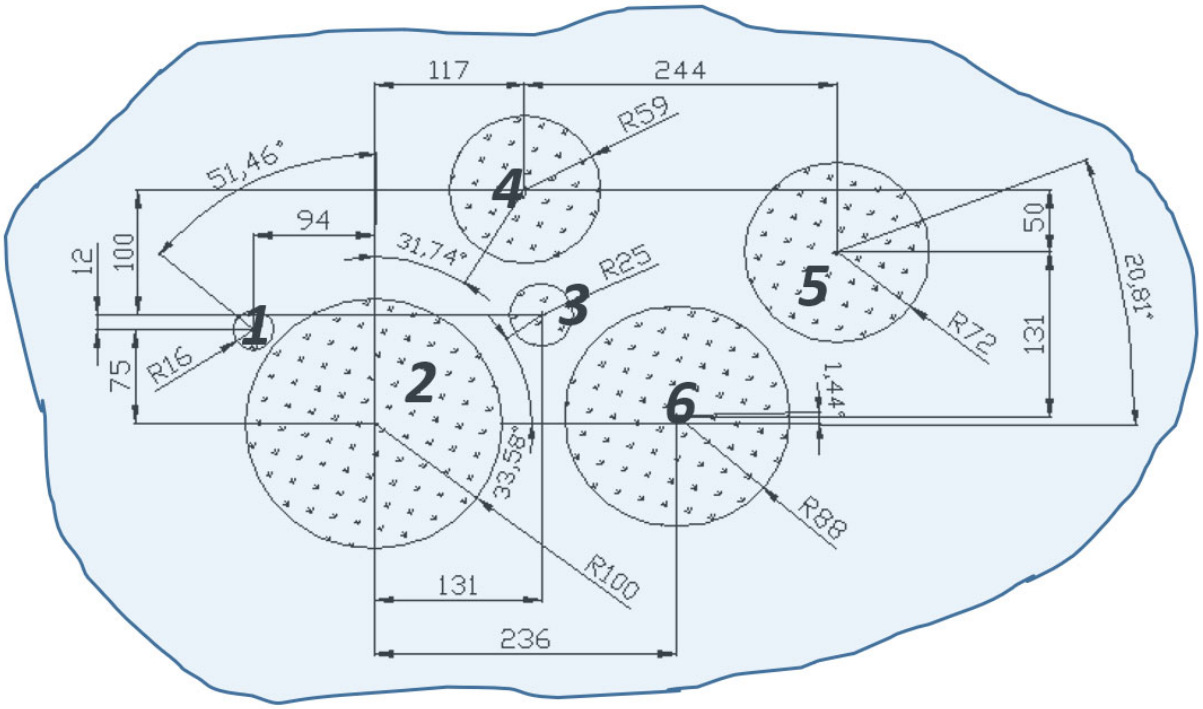

Fig. 6. To the computational model of crushing drops of the dispersed phase of the emulsion (characteristic sizes in microns)

The calculation results are shown in Figs. 7-8, where the moments of droplet merging are visible: first, №2 with 3, then №4 with 5, then №2 with 4, etc. At the moment of the merging of two drops, after the formation of a new drop, the acceleration of the oil-vapour interface increases abruptly (Fig. 7b), which is explained by a sharp decrease in the Laplace force, which is included in the Rayleigh-Plesset equation, due to a sharp increase in the radius of the interface. Temperature and vapour pressure have almost similar patterns of change. The heat flux from oil to steam (Fig. 8) can have a resulting value, both between the two initial ones and higher than the largest of the initial ones, which the determination value of the radius of the formed particle can explain.

For example, for $\tau \approx 6 \cdot 10^{-5}$ s, when droplets No. 4 and 5 merge, one can see an increase in the radius and heat flux. Abrupt changes in acceleration and velocity values can cause hydrodynamic instability of neighbouring drops. But, in this case, as the calculation showed, the magnitudes of these forces caused by g and w are insufficient for crushing nearby drops. The calculation was performed according to the method given in (Zevnik & Dular 2020, Janssen & Kulacki 2017, Prajapat & Gogate 2019). The heat flux varies inversely with the steam temperature.

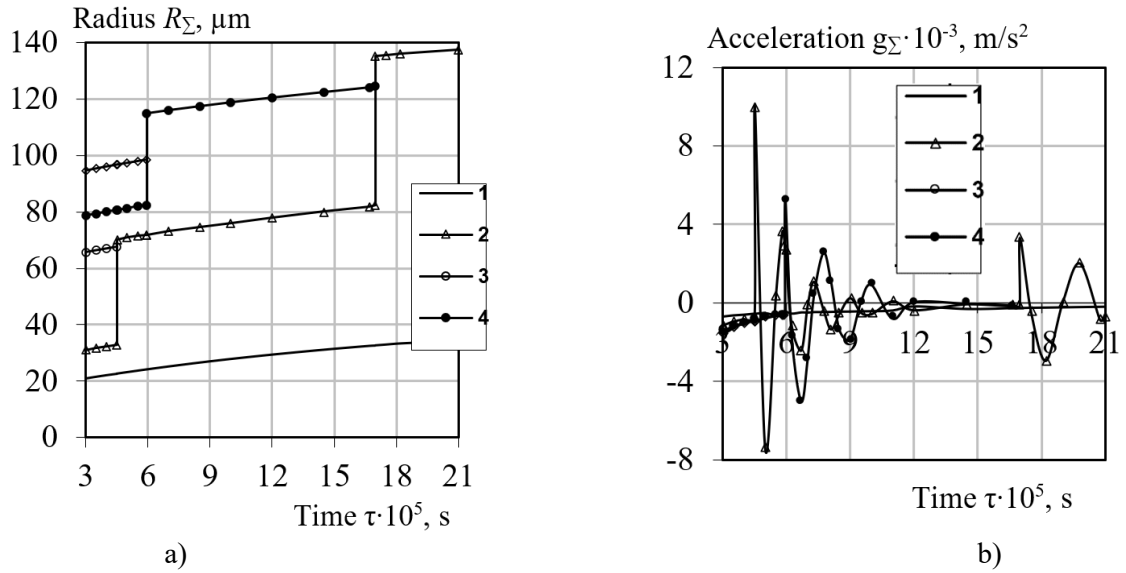

Fig. 7. Change in droplet radius (a) and the acceleration of the oil-steam interface (b) with time as a result of the formation of a conglomerate, 1, 2, 3, 4 – numbers of drops of the dispersed phase indicated in Fig. 6

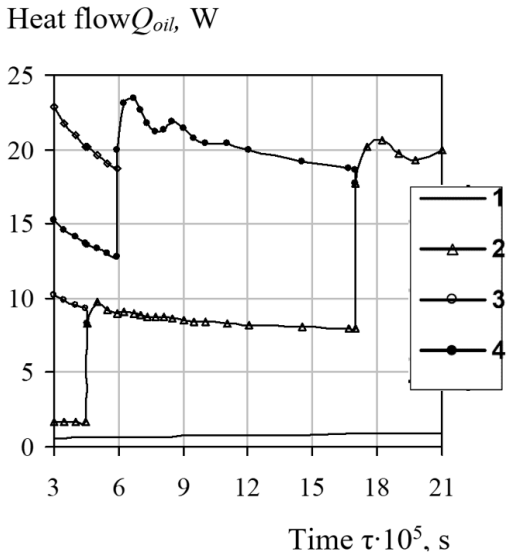

Fig. 8. The change in the heat flux from oil to steam in time during the coalescence of drops (notation from Fig. 7a), 1, 2, 3, 4 – numbers of drops of the dispersed phase indicated in Fig. 6

Thus, this assessment of the thermodynamic and, consequently, hydrodynamic instability of the emulsion flow makes it possible to obtain a general picture of changes in the emulsion structure and the intensity of HMT processes. Of course, the assumption that the drops merge instantly leads to somewhat incorrect results, but the question of the time two drops of different sizes merge also remains open. The coalescence time of two drops of various sizes, calculated by the average radius and the method (Merzkirch et al. 2015, Nigmatulin et al. 2004, Nhut et al. 2015), is $\Delta\tau \approx 7^{-7}$ s, which practically coincides with the calculation step. Another variant of the boiling scheme is also possible, in which the drops do not merge but grow, interacting with each other, if the stabilising effect of the surfactant is sufficiently large. However, a combination of these schemes can also exist. Generally, any scheme of consideration will lead to thermal equilibrium, both if we consider the merger and study the thermal contact. Therefore, this method is quite acceptable for calculating the boiling of emulsions.

4. Conclusions

1. The developed model of disintegration of a drop of a dispersed phase, surrounded by many neighbouring boiling particles, makes it possible to determine, in terms of force, the dynamic effect that leads to fragmentation, deformation, or displacement of the drop under consideration. The main differences in consideration of the processes of crushing boiling and nonboiling drops of the dispersed phase of the emulsion are indicated. The calculation proved that for boiling particles, it is necessary to consider two maxima of the forces acting from neighbouring boiling particles while determining the main one from them. It is possible to use this model to determine the ongoing crushing processes and the time scale of the action of forces that lead to the destruction of drops.
2. The proposed models for the movement and coalescence of dispersed phase droplets characterise the main processes that occur during the boiling of emulsion media. The movement of drops is ambiguous, as evidenced by the constantly changing angle of particle movement in space, which, in turn, indicates a complex hydrodynamic situation in the volume of the emulsion. At low temperatures (corresponding to pressure drops), the displacement of droplets relative to their initial location can be neglected. The possibility of using the processes of movement and merging of dispersed phase droplets to crush either the moving drop itself or neighbouring ones that are near the conglomerate formed at the moment of the merger is indicated.
3. The most probable mechanisms of nucleation, boiling, and destruction of superheated droplets of a low-boiling dispersed phase of a liquid emulsion have been analysed. Relations are obtained that determine the specific heat flux from the heating surface cooled by a boiling dilute emulsion.
4. The resonant mechanism of destruction of low-boiling droplets of the dispersed phase by steam bubbles is substantiated, which is one of the possible consequences of the joint transfer of momentum and heat in emulsions.

All of the described processes are the main mechanisms for increasing the intensity of heat and mass transfer, both in the volume of the boiling emulsion and on the heating contact surfaces of heat exchangers.

References

Adhikari, Ram, Chandra, Vaz, Jerson, Wood, David. (2016). Cavitation Inception in Crossflow Hydro Turbines. *Energies*, *9*(4), 237. https://doi.org/10.3390/en9040237.

Albanese, L., Baronti, S., Liguori, F., Meneguzzo, F., Barbaro, P., Vaccari, F.P. (2019). Hydrodynamic cavitation as an energy-efficient process to increase biochar surface area and porosity: A case study. *Journal of Cleaner Production*, *210*, 159-169. https://doi.org/10.1016/j.jclepro.2018.10.341

Badve, M.P., Alpar, T., Pandit, A.B., Gogate, P.R., Csoka, L. (2015). Modeling the shear rate and pressure drop in a hydrodynamic cavitation reactor with experimental validation based on KI decomposition studies. *Ultrasonics Sonochemistry*, *22*, 272-277. https://doi.org/10.1016/j.ultsonch.2014.05.017

Bao, Ngoc, Tran, Haechang, Jeong, Jun-Ho, Kim, Jin-Soon, Park, Changjo, Yang. (2020). Effects of Tip Clearance Size on Energy Performance and Pressure Fluctuation of a Tidal Propeller Turbine. *Energies*, *13*, 4055. https://doi.org/10.3390/en13164055.

Chandrapala, J., Oliver, C., Kentish, S., Ashokkumar, M. (2012). Ultrasonics in food processing – food quality assurance and food safety. *Trends in Food Science & Technology*, *26*(2), 88-98. https://doi.org/10.1016/j.tifs.2012.01.010

Chernin, Leon, Val, Dimitri, V. (2017). Probabilistic prediction of cavitation on rotor blades of tidal stream turbines. *Renewable Energy*, *113*, 688-696. https://doi.org/10.1016/j.renene.2017.06.037

Dąbek, L., Kapjor, A., Orman, Ł.J. (2018). *Boiling heat transfer augmentation on surfaces covered with phosphor bronze meshes*. Proc. of 21st Int. Scientific Conference on The Application of Experimental and Numerical Methods in Fluid Mechanics and Energy 2018, MATEC Web of Conferences, 168, 07001. https://doi.org/10.1051/matecconf/201816807001

Dąbek, L., Kapjor, A., Orman, Ł.J. (2019). Distilled water and ethyl alcohol boiling heat transfer on selected meshed surfaces. *Mechanics & Industry*, *20*, 701. https://doi.org/10.1051/meca/2019068

Dietzel, Dirk, Hitz, Timon, Munz, Claus-Dieter, Kronenburg, Andreas. (2017). *Expansion rates of bubble clusters in superheated liquids*. Polytechnic University of Valencia Congress, ILASS2017. 28th European Conference on Liquid Atomization and Spray Systems, 6-8 September 2017, Valencia, Spain. http://dx.doi.org/10.4995/ILASS2017.2017.4714

Feng, Jie, Muradoglu, Metin, Kim, Hyoungsoo, Ault, Jesse, T., Stone, Howard, A. (2016). Dynamics of a bubble bouncing at a liquid/liquid/gas interface. *Journal of Fluid Mechanics*, *807*, 324-352. https://doi.org/10.1016/j.ultrasmedbio.2005.02.007

Ganesan, Balasubramanian, Martini, Silvana, Solorio, Jonathan, Walsh, Marie, K. (2015). Determining the Effects of High Intensity Ultrasound on the Reduction of Microbes in Milk and Orange Juice Using Response Surface Methodology. *International Journal of Food Science*, *2015*, Article ID 350719. https://doi.org/10.1155/2015/350719

Gasanov, B.M., Bulanov, N.V. (2015). Effect of the droplet size of an emulsion dispersion phase in nucleate boiling and emulsion boiling crisis. *International Journal of Heat and Mass Transfer*, *88*, 256-260. https://doi.org/10.1016/j.ijheatmasstransfer.

Janssen, D., Kulacki, F.A. (2017). Flow boiling of dilute emulsions. *International Journal of Heat and Mass Transfer*, *115*, Part A, 1000-1007. https://doi.org/10.1016/j.ijheatmasstransfer.2017.07.093

Koshlak, H., Pavlenko, A. (2019). Method of formation of thermophysical properties of porous materials. *Rocznik Ochrona Srodowiska*, *21*(2), 1253-1262.

Merzkirch, W., Rockwell, D., Tropea, C. (2015). *Orifice Plates and Venturi Tubes*. Cham; Heidelberg; New York, NY; Dordrecht; London: Springer International Publishing. Available online at: https://link.springer.com/content/pdf/bfm%3A978-3-319-16880-7%2F1.pdf

Nhut, Pham-Thanh, Hoang, Van, Tho, Young, Jin, Yum. (2015). Evaluation of cavitation erosion of a propeller blade surface made of composite materials. *Journal of Mechanical Science and Technology*, *29*, 1629-1636.

Nigmatulin, R., Taleyarkhan, R., Lahey, R. (2004). Evidence for nuclear emissions during acoustic cavitation revisited. *Journal of Power and Energy*, *218*, Part A: J. Power and Energy. https://doi.org/10.1243/0957650041562208

Pavlenko, A., Koshlak, H., Usenko, B. (2014a). The processes of heat and mass exchange in the vortex devices. *Metallurgical and Mining Industry*, *6*(3), 55-59.

Pavlenko, A., Koshlak, H., Usenko, B. (2014b). Heat and mass transfer in fluidised layer. *Metallurgical and Mining Industry*, *6*(6), 96-100.

Pavlenko, A.M. (2018). Dispersed phase breakup in boiling of emulsion. *Heat Transfer Research*, *49*(7), 633-641, https://doi.org/10.1615/HeatTransRes.2018020630.

Pavlenko, A.M. (2019). Energy conversion in heat and mass transfer processes in boiling emulsions. *Thermal Science and Engineering Progress*, *15*, 1-8. https://doi.org/10.1016/j.tsep.2019.100439

Pavlenko, A.M., Koshlak, H. (2021). Application of thermal and cavitation effects for heat and mass transfer process intensification in multicomponent liquid media. *Energies*, *14*(23), 7996. https://doi.org/10.3390/en14237996

Prajapat, A.L., Gogate, P.R. (2019). Depolymerisation of carboxymethyl cellulose using hydrodynamic cavitation combined with ultraviolet irradiation and potassium persulfate. *Ultrasonics Sonochemistry*, *51*, 258-263. https://doi.org/10.1016/j.ultsonch.2018.10.009

Sun, X., Wang, Z., Xuan, X., Ji, L., Li, X., Tao, Y., Boczkaj, G., Zhao, S., Yoon, J.Y., Chen, S. (2021). Disinfection characteristics of an advanced rotational hydrodynamic cavitation reactor in pilot scale. *Ultrasonics Sonochemistry*, *73*, 105543. https://doi.org/10.1016/j.ultsonch.2021.105543.

Xun, Sun, Songying, Chen, Jingting, Liu, Shan, Zhao, Joon, Yong, Yoon. (2020). Hydrodynamic Cavitation: A Promising Technology for Industrial-Scale Synthesis of Nanomaterials. *Front. Chem.*, *15*. https://doi.org/10.3389/fchem.2020.00259

Zevnik, Jure, Dular, Matevž, (2020). Cavitation bubble interaction with a rigid spherical particle on a microscale. *Ultrasonics Sonochemistry*, *69*, 105252. https://doi.org/10.1016/j.ultsonch.2020.105252